

Three-dimensional Ginzburg-Landau simulation of a vortex line displaced by a zigzag of pinning spheres

Mauro M. Doria* and Antonio R. de C. Romaguera†

Instituto de Física, Universidade Federal do Rio de Janeiro

C.P. 68528, 21941-972, Rio de Janeiro RJ, Brazil

Welles A. M. Morgado‡

Instituto de Física, Pontifícia Universidade Católica do Rio de Janeiro

C.P. 38071, 22452-970, Rio de Janeiro RJ, Brazil

Abstract

A vortex line is shaped by a zigzag of pinning centers and we study here how far the stretched vortex line is able to follow this path. The pinning center is described by an insulating sphere of coherence length size such that in its surface the de Gennes boundary condition applies. We calculate the free energy density of this system in the framework of the Ginzburg-Landau theory and study the critical displacement beyond which the vortex line is detached from the pinning center.

PACS numbers: 74.80.-g Spatially inhomogeneous structures, 74.25.-q General properties; correlations between physical properties in normal and superconducting states, 74.20.De Phenomenological theories (two-fluid, Ginzburg-Landau, etc.)

Keywords: Ginzburg-Landau, Tridimensional, pinning theory

I. INTRODUCTION

The basic idea of pinning theory is that the vortex is not rigid but adjustable to a local distribution of defects^{1,2,3}. In this paper we consider a vortex line pinned by a zigzag of pinning centers that are insulating spheres of radius R of the order of the coherence length ξ . The de Gennes boundary condition⁴ applies at the pinning sphere surface, considered as an insulator-superconductor interface. The straight line connecting these pinning centers is a path with abrupt right and left turns, whose zigzag fits into a single plane. As pointed out by Yu. N. Ovchinnikov⁵ long ago, the investigation of various types of inclusions in superconducting materials is of particular interest because of the onset of metastable states. We have already considered a similar vortex depinning transition⁶ to the one considered here which is being reviewed from the point of view of displaced defects.

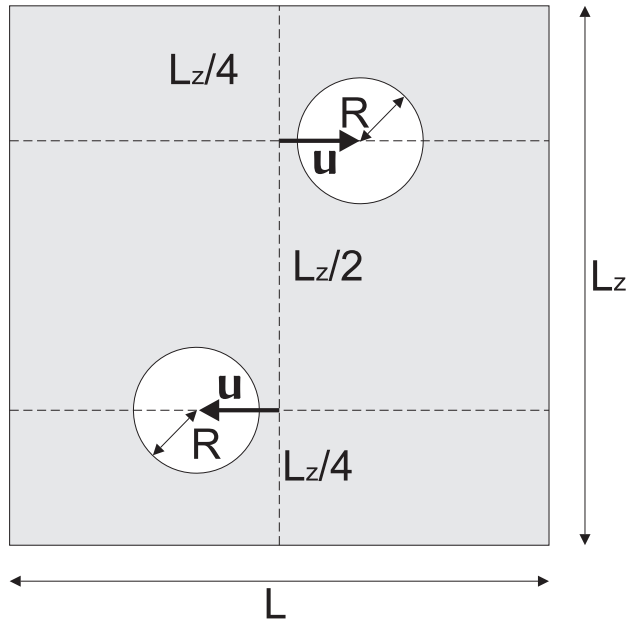


FIG. 1: Schematic view of the unit cell middle plane. This view captures the displaced pinning spheres of radius R displaced by u along the x direction. The unit cell is orthorhombic with base side L and height L_z .

An energetic balance makes the vortex line follows this zigzag path as long as trapping by the pinning spheres is advantageous as compared to the increase in length caused by the zigzag path. There is a critical path that sets a depinning transition beyond which the stretched vortex line is no longer able to follow the zigzag path of the pinning centers.

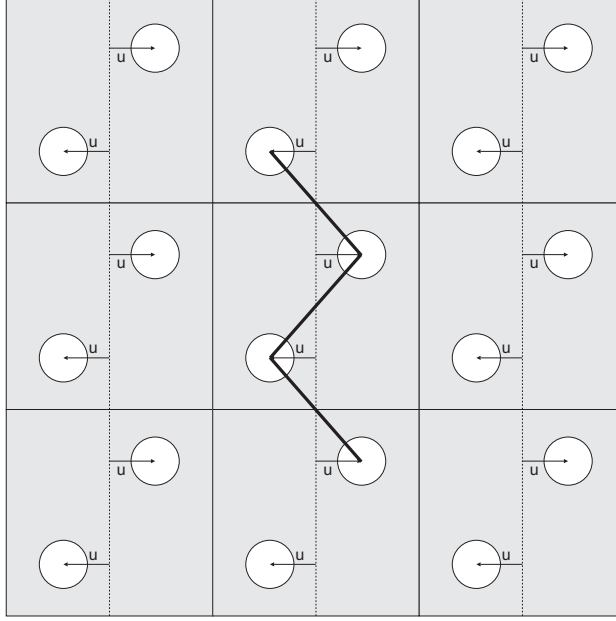


FIG. 2: Nine equivalent unit cells are patched together here and the dark line connecting some pinning spheres shows the zigzag path followed by the vortex.

This critical path is associated to a critical displacement u_c that we determine in this paper through numerical simulations of the Ginzburg-Landau theory⁷. From the point of view of the Ginzburg-Landau theory, pinning may be caused either by spatial fluctuations of the critical temperature, $T_c(\vec{x})^1$, or by the mean free-path that changes the coefficient in front of the gradient term, $\xi(\vec{x})^2|(\vec{\nabla} - \frac{2\pi i}{\Phi_0}\vec{A})\Delta|^2$. The interaction between a vortex line and a pinning center has been considered by many authors in the context of the Ginzburg-Landau theory^{8,9,10,12}. In this paper we only consider the no magnetic shielding limit, such that the field penetrates in the superconductor and there is no Meissner-Ochsenfeld effect. This situation can be viewed as a large κ limit, $\kappa = \lambda/\xi$ being the dimensionless Ginzburg-Landau parameter and λ is the penetration depth.

The z -axis is the direction of the magnetic induction, and so, of the applied magnetic field, and perpendicular to it is the x -axis. In case of no defects, the vortex is a straight line oriented along the z -axis. The defects are equally spaced along the z axis and assume alternate displacements u and $-u$ along the x axis. Although the zigzag of defects fit into a single plane the problem is genuinely three-dimensional because the defects are coherence length size spheres. Consider the position of two defects, $(L/2 - u, L/2, Lz/4)$ and $(L/2 + u, L/2, Lz/4)$. All others are obtained from these two forming an infinite lattice in the x, y

and z directions. The position of the all others defects can be obtained by translation of L along the x or y axis and by Lz along the z axis. The periodicity due to the zigzag of defects allow to describe this system through a orthorhombic unit cell of height Lz , and of square basis $Lx = Ly = L$, with two pinning centers inside, at the above positions $(L/2 - u, L/2, Lz/4)$ and $(L/2 + u, L/2, 3Lz/4)$ with respect to a coordinate frame whose origin is at the left-down corner of the unit cell. Figures 1 and 2 give a pictorial view of the geometrical arrangement of pinning centers inside the superconductor which is under investigation here.

The numerical results obtained from simulations of the Ginzburg-Landau theory yield the order parameter in each point of space. These results are visualized as iso-surfaces of the density, that is of the modulus of the order parameter squared, taken at a fixed value, as shown in figures 3 and 4. Notice that figure 4 corresponds to nine equivalent unit cells, as shown in figure 3, patched together. Many other possible pinned vortex configurations are

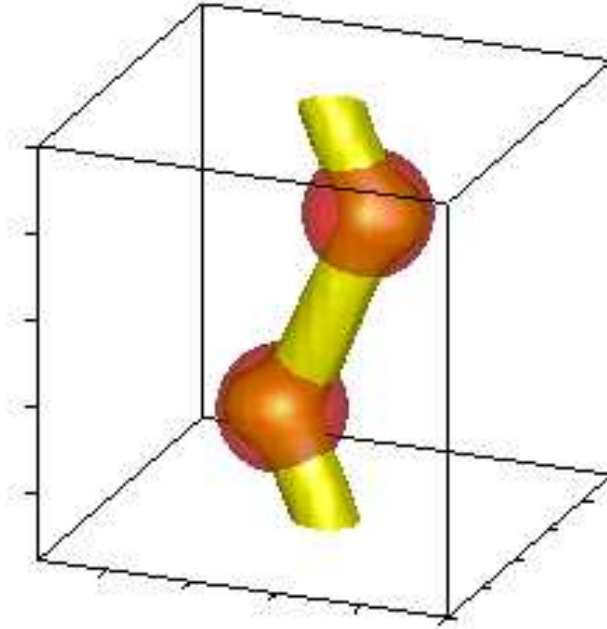


FIG. 3: The vortex line remains pinned by the two displaced insulating spheres of radius $R = 1.8\xi$ in an unit cell with $L = Lz = 12\xi$. The picture is the isosurface $|\Delta|^2 = 0.2507$, which means a density value approximately one fourth of its maximum value. The pinning spheres are shown in dark gray color.

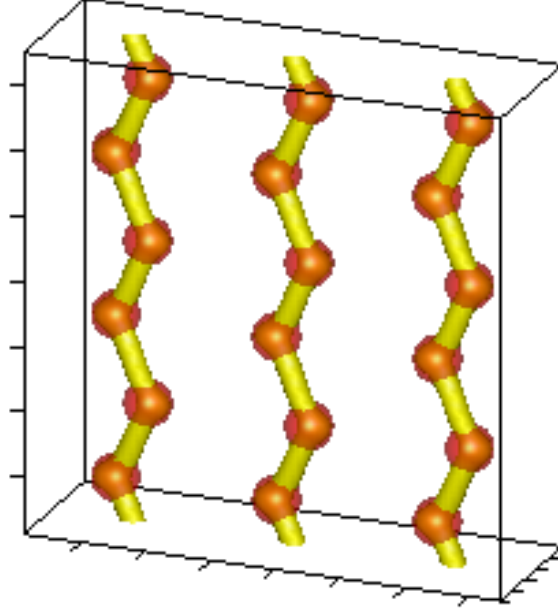


FIG. 4: Nine equivalent unit cells are patched here displaying the vortex lines pinned by the spheres, as described in figure 3.

possible in the pinning center arrangement displayed in figure 2. Figure 4 gives one among many other, but it is the only one described by the unit cell of figure 3. However these other possibilities are not considered here, although the present method is able to treat them by searching vortex configurations in larger unit cells containing several pairs of pinning centers. We restrict our study here to the minimum deviation of the vortex from the straight line, which is well described by the present choice of unit cell. The present study involves some parameters related to the unit cell, L_z and L , and to the pinning center, u and R . The unit cell basis is fixed to $L = 12\xi$, and so our goal is to numerically obtain the Helmholtz free energy $F(u, Lz, R)$. For each point we obtain a density plot such as shown in figure 3. This paper is organized as follows. In section II, we discuss out theoretical approach. In sections III we show the results obtained through numerical simulations. In section IV we summarize the main results of the work.

II. THEORETICAL APPROACH

We find numerical solutions of the Ginzburg-Landau theory in the unit cell using a mesh grid to describe it^{8,9,10}. The distance between two consecutive mesh points, a , is equal to 0.5ξ , consistent to the fact that a must be smaller than the coherence length ξ , which is the minimum physical scale of the Ginzburg-Landau theory. Thus the number of mesh points describing the unit cell square basis is P^2 , and so $P = 25$ since $L = a(P - 1)$. Notice that the pinning sphere also imposes a limit on the mesh parameter which cannot be larger than the pinning center radius, that is $a = 0.5\xi < R$, otherwise there will be one or no mesh point describing the pinning region. In this case the order parameter does not vanish inside the defect but just undergoes a drop on its value. The energy density functional of the Ginzburg-Landau theory⁷ is expressed in units of the critical field energy density¹⁰, $H_c^2/4\pi$ and the order parameter density, $|\Delta|^2$ is dimensionless, varying between 0 and 1. The concept of unit cell brings a periodicity to the problem, and so the search for the free energy minimum must be done under a constraint, the number of vortices inside the unit cell, $\vec{\nu}\phi_0$, described by integers: $\vec{\nu} = n_x\hat{x} + n_y\hat{y} + n_z\hat{z}$. The magnetic induction, which is the average of the local field taken over the unit cell volume, $\vec{B} = \int_v \vec{h} d^3r/V$, has a relationship to these integers, and in reduced units is $\vec{B}(\vec{x}) = 2\pi\kappa\xi^2(n_x\hat{x}/L.L_z + n_y\hat{y}/L.L_z + n_z\hat{z}/L^2)$. In the present paper we only consider a single vortex oriented along the z -axis, hence $\vec{\nu} = \hat{z}$.

$$F = \int \frac{dv}{V} \tau(\vec{x}) \left[\xi^2 \left| \left(\vec{\nabla} - \frac{2\pi i}{\Phi_0} \vec{A} \right) \Delta \right|^2 - |\Delta|^2 \right] + \frac{1}{2} |\Delta|^4, \quad (1)$$

The function $\tau(\vec{x})$ is a step-like function used to describe the pinning spheres in this approach¹⁰. Explicitly we have $\tau(\vec{x}) = \tau_1(\vec{x})\tau_2(\vec{x})$ and

$$\tau_i(\vec{x}) = 1 - \frac{2}{1 + e^{(|\vec{x} - \vec{x}_i|/R)^N}}, \quad (2)$$

where τ_i is equal to 0 inside and 1 outside the i th sphere. The above explicit representation of the τ function is necessary for computational reasons and for accuracy we take that $N = 8$. In the limit $N \rightarrow \infty$, the function τ tends to the well-known Heaviside function, $\tau(\vec{x}) = \Theta\left(\frac{|\vec{x} - \vec{x}_1|}{R} - 1\right) \Theta\left(\frac{|\vec{x} - \vec{x}_2|}{R} - 1\right)$. The most significant advantage of the present method, is that the free energy functional, Eq. 1, contains the appropriate boundaries conditions to the problem. This removes the necessity of solving the theory in two independent regions and later applying the Neumann boundary conditions. Besides the present method easily

applies to internal regions of any shape, not just spherical, and finds its solution for the given normal-superconductor interface¹⁰.

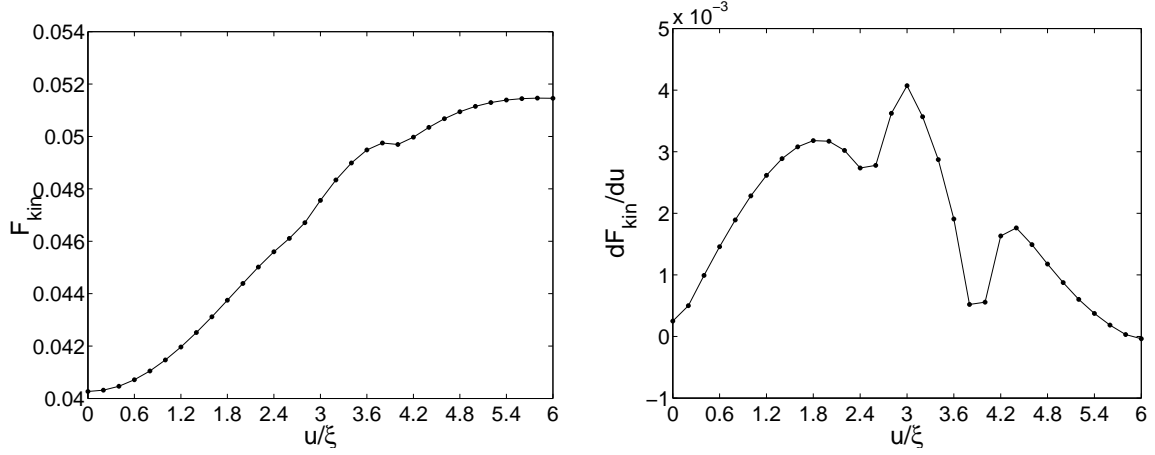


FIG. 5: Kinetic energy and its derivative in the left and right part of the figure, respectively. The valleys in the derivative are associated to depinning. The critical displacement is associated to the minimum in these valleys. The pinning sphere radius is $R = 1.8\xi$ and $L = Lz = 12\xi$

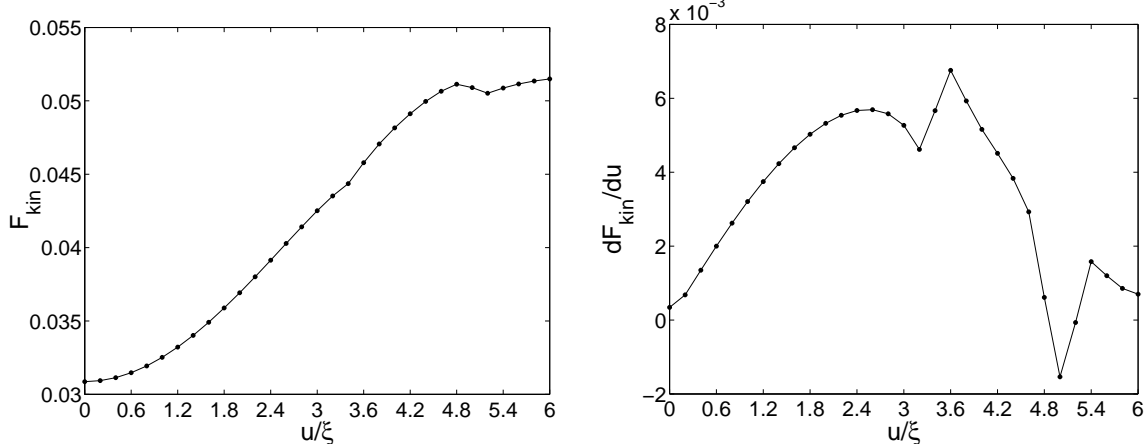


FIG. 6: The kinetic energy and its derivative for a system with $R = 2.4\xi$, $L = Lz = 12\xi$ similar to figure 5. Thus the critical displacement depends on the radius of the defect.

Since we are in the no shielding limit, the vector potential $\vec{A}(\vec{x})$ is determined from the condition of magnetic flux quantization inside the unit cell. The vector potential does not participate in the minimization process of the free energy density that only takes into account the real and imaginary parts of the order parameter. The free energy density contains two terms. The first term is the condensation energy density, $-\tau(\vec{x}) |\Delta|^2 + \frac{1}{2} |\Delta|^4$, which in case

of no vortices ($|\Delta|^2 = 1$) and no pinning sphere ($\tau = 1$) has the value -0.5. The presence of a pinning sphere raises the energy since inside it the density vanishes ($|\Delta|^2 = 0$). And the second term, the kinetic energy density, $\tau(\vec{x})\xi^2 \left| (\vec{\nabla} - \frac{2\pi i}{\Phi_0} \vec{A}) \Delta \right|^2$. Notice that there is kinetic energy in case of no vortices but with a defect. At the insulating-superconducting interface τ changes from 1 to 0 and this causes a bending of the order parameter, which has some kinetic energy cost.

III. RESULTS

The critical displacement u_c is better observed in the derivative of the kinetic energy density⁶. Figures 5 and 6 shows the curves dF_{kin}/du versus u for two selected radii, namely $R = 1.8\xi$, and $R = 2.4\xi$, respectively, and in both cases a double hump structure with a local minimum between them is seen. For growing displacement u the first minimum of the kinetic energy density occurs for no displacement and the second minimum corresponds to the depinning transition u_c . After the second hump there is a third minimum associated to the depinning from the second sphere. Thus detachment of the vortex from a pinning sphere makes the kinetic energy density reach a minimum. To understand this consider the local maximum that precedes the detachment. For small u the vortex core is superposed to the two pinning centers. As long as the vortex is pinned by the two spheres, and follows the zigzag path, the order parameter has to adjust around one single common interface that involves both the vortex core and the pinning centers. The maximum stretch of the vortex line is the longest zigzag path, a configuration that demands the maximum amount of circulating current around the vortex. Thus the maximum stretch of the vortex line is achieved when the kinetic energy reaches its maximum.

Beyond the maximum stretch the vortex unpins from one of the spheres, and the kinetic energy decreases for further displacement u . Consequently one expects that the kinetic energy undergoes a minimum because following the detachment of the first pinning center from the vortex core the kinetic energy must rise again. Notice that in case of the nucleation of two independent surfaces from a single one the deflection of the order parameter must be taken into account in each one of the new nucleated surfaces. This nucleation leads to an extra growth of the kinetic energy because there is a gradient of the order parameter in the interfaces. The total interface area has grown because there are two surfaces instead of just one after the nucleation. Here the two interfaces are the $z = L_z/4$ pinning sphere and the other one formed by the $z = 3L_z/4$ pinning center together with the vortex core. The depinning transition is shown in figure 7 that shows a sequence of increasing u displacements that lead to the depinning of the vortex line from the zigzag path. The same sequence is

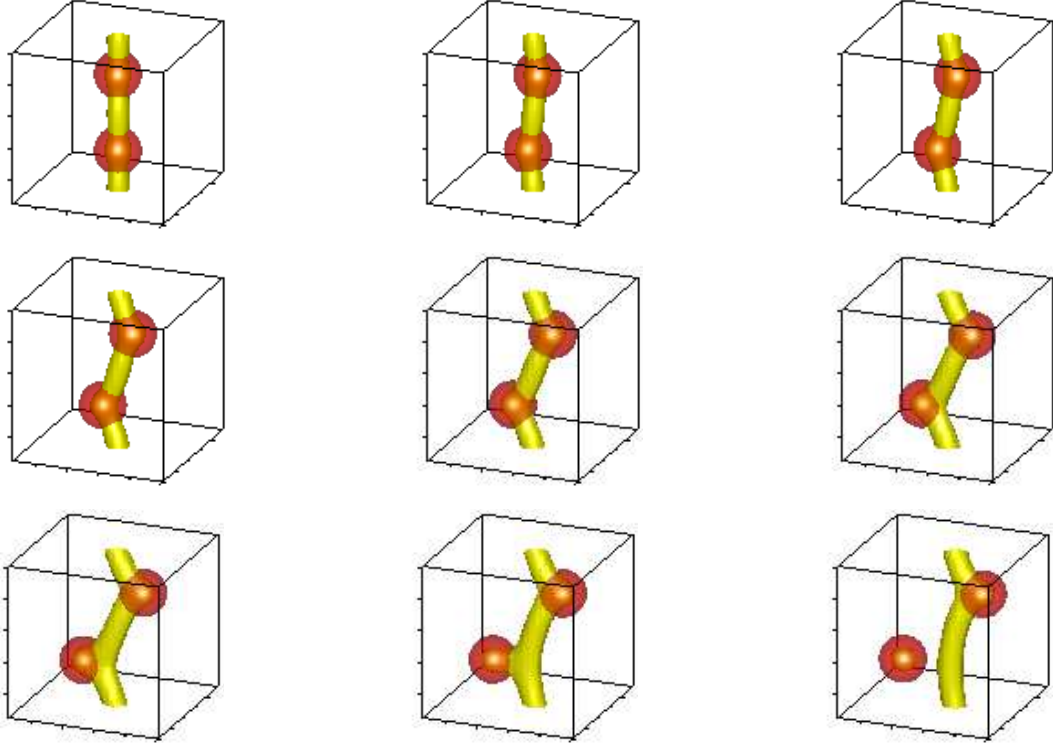


FIG. 7: Sequence of views of the vortex line for several growing displacements u/ξ equal to 0.0, 0.4, 0.8, 1.2, 1.6, 2.0, 2.4, 2.8, and 3.2. The unit cell is cubic, $L_z = L = 12\xi$, and the pinning center is $R = 1.8\xi$. The isosurfaces are taken at a density approximately equal for all cases, namely, one fourth of its maximum value, $|\Delta|^2 \approx 0.25$.

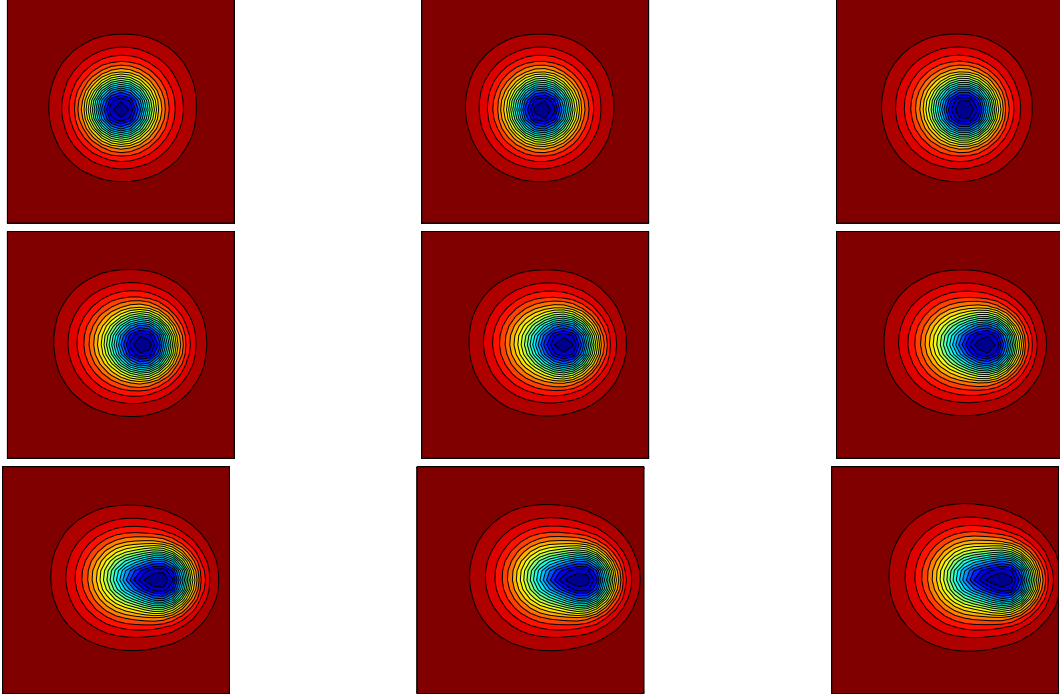


FIG. 8: The same sequence of views of figure 7 is shown here through $z = 3L_z/4$ cuts of that unit cell ($L = L_z = 12\xi, R = 1.8\xi$). For the displacement $u = 3.2\xi$, the vortex line is still pinned by upper the sphere.

shown again through contour lines along the two planes that cross the pinning spheres in half, $z = L_z/4$ (figure 9) and $3L_z/4$ (figure 9).

The behavior of the free energy density versus the displacement u is shown in figure 10 for several radii, ranging from $R = 1.2\xi$ to 2.8ξ , and for a cubic unit cell $L = L_z = 12\xi$. The left graphic in the figure 12 exhibits the dependency of the critical displacement u_c with the radius of the spheres. Due to our choice of unit cell parameter L , R is limited to the interval $1.0\xi < R < 3.0\xi$, otherwise are smaller than the vortex core or the pinning spheres will not fit in the unit cell.

The critical displacement is dependent on the height of the unit cell L_z , as shown in figures 11 and in the right side of the figure 12 for the case that $R = 2.0\xi$. Figure 11 shows a set of free energy density curves versus L_z associated to different u displacements in steps of 0.2ξ , ranging from 0 to 6.0ξ in the crescent sequence indicated by the arrow. The 0 displacement curve is the lowest in energy and the 6.0ξ is the largest, in agreement with the idea that large pinning centers increase the energy since they bring non-superconducting

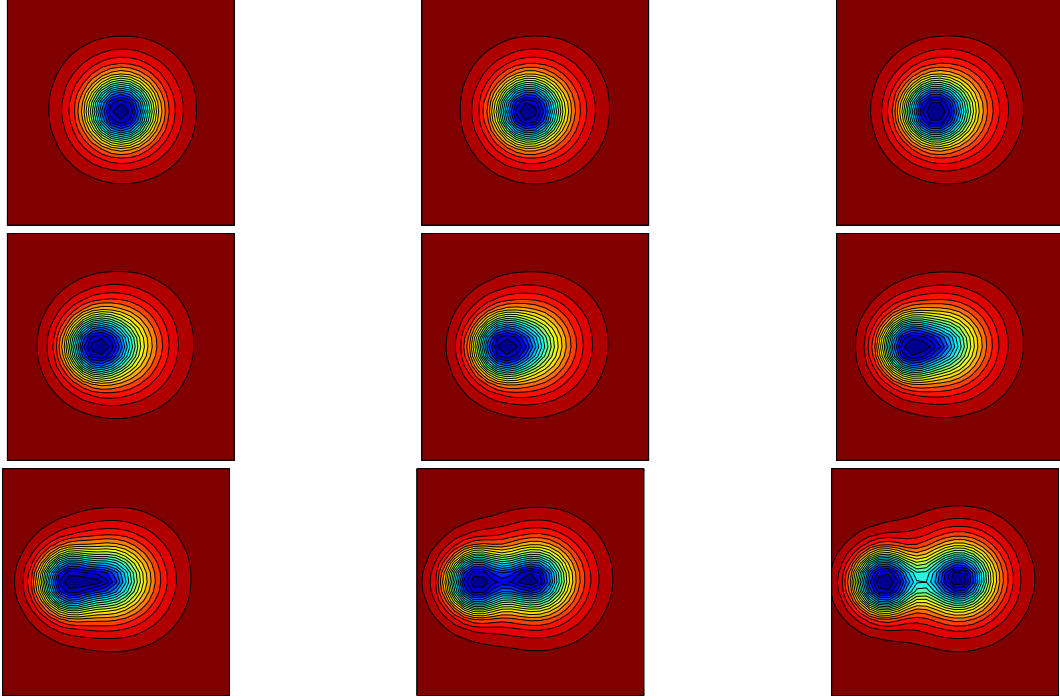


FIG. 9: The same sequence of views of figure 7 is shown here through $z = L_z/4$ cuts of that unit cell ($L = L_z = 12\xi, R = 1.8\xi$). For the displacement $u = 3.2\xi$, the vortex line is detached from the lower sphere.

regions to the unit cell. The right side of Figure 12 shows that unit cells with increasing L_z allow for larger critical displacements. The zigzag of pinning centers is not so demanding of the vortex line for large L_z , and so, we expect that large displacements are possible in these cases, as confirmed by figures 11 and 12.

IV. CONCLUSIONS

The study of the interaction among pinning centers and vortices is crucial to the understanding of type II superconductors. For this reason artificially made pinning centers are useful and many kinds have been fabricated^{13,14,15,16,17} though not of the kind considered here. In this paper the Ginzburg-Landau theory was numerically solved on a three-dimensional mesh to study properties of a vortex line near a zigzag of pinning centers. The pinning centers are insulating spheres of coherence length size and the system was described by an orthorhombic unit cell containing two displaced defects. We find that there is a critical displacement above which the vortex line is detached from a pinning center. Below this

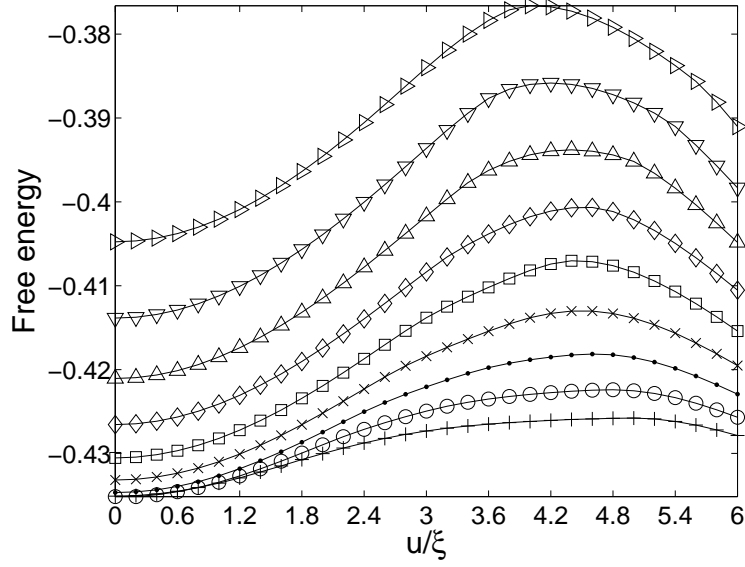


FIG. 10: The free energy versus the pinning sphere dislocation for different radii, all obtained for a cubic unit cell with $L_z = L = 12\xi$. The symbols $+$, \circ , \bullet , \times , \square , \diamond , \triangle , ∇ and \triangleright mean the radius R/ξ equal to 1.2, 1.4, 1.6, 1.8, 2.0, 2.2, 2.4, 2.6 and 2.8 respectively. The line of critical displacement u_c is also shown here. The vortex remains pinned to the zigzag of defects only for $u < u_c$.

transition the vortex line is pinned by both defects and above by just one. The study of

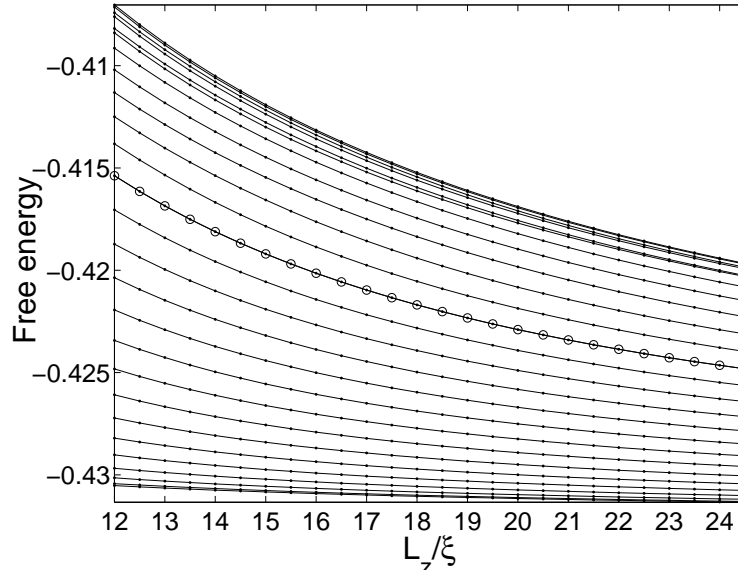


FIG. 11: Several $F(u, L_z, R = 2.0\xi) \times L_z$ curves, associated to different u displacements, are shown here. The arrow indicate the ascending values of u , ranging 0.0 to 6.0ξ with a step of 0.2ξ . For reference the $u = 2.8\xi$ curve has its points magnified here.

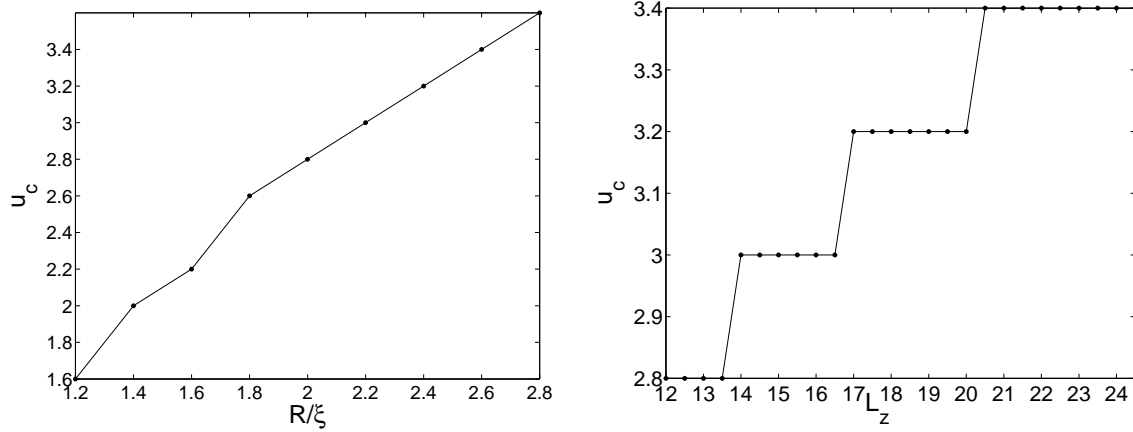


FIG. 12: In the left side, the dependence of u_c with the radius of the sphere is shown ($L = L_z = 12\xi$). In the right side, the dependence of u_c with the height L_z is presented for a defect of radius $R = 2.0\xi$.

coherence length size defects may also be found useful in some other situations. Recently it has been shown that the nucleation of such defects is a mechanism to lower the energy of the superconducting state¹¹.

V. ACKNOWLEDGMENTS

Research supported in part by Instituto do Milênio de Nano-Ciências, CNPq, and FAPERJ (Brazil).

* Electronic address: mmd@if.ufrj.br

† Electronic address: ton@if.ufrj.br

‡ Electronic address: welles@if.puc-rj.br

¹ A. I. Larkin, Sov. Phys.-JETP 31, 784,1970.

² E. H. Brandt, Rep. Prog. Phys. 58, 1465, 1995.

³ J. B. Ketterson and S. N. Song, Superconductivity, Cambridge University Press, 1st. edition, Cambridge,UK, 1999.

⁴ P. G. de Gennes, Superconductivity in Metals and Alloys, Persus Book, 2nd. edition, Massachusetts,1989.

- ⁵ Yu. N. Ovchinnikov, Soviet Physics - JETP 52, 755, 1980; Soviet Physics - JETP 57, 1162, 1982; and Soviet Physics - JETP 57, 136, 1983.
- ⁶ Antonio R. de C. Romaguera and M. M. Doria, Eur. Phys. Jour. B 42, 3, 2004.
- ⁷ A. A. Abrikosov, Soviet Physics JETP 5, 1174, 1957.
- ⁸ M. M. Doria and Sarah C. B. Andrade, Phys. Rev. B 60, 13164, 1999.
- ⁹ M. M. Doria and Gilney F. Zebende, Brazilian J. Phys. 32, 690, 2002.
- ¹⁰ M. M. Doria and Gilney F. Zebende, Phys. Rev. B 66, 064519, 2002.
- ¹¹ M. M. Doria and Antonio R. de C. Romaguera, Eur. Phys. Lett. 67, 446, 2004.
- ¹² D. J. Priour and H. A. Fertig, Phys. Rev. B 67, 054504, 2003.
- ¹³ A. Bezryadin and B. Pannetier, J. of Low Temp. Phys 98, 251, 1995.
- ¹⁴ J. Y. Lin, M. Gurvitch, S. K. Tolpygo, A. Bourdillon, S. Y. Hou and Julia M. Phillips, Phys. Rev. B 54, R12717, 1996.
- ¹⁵ V. V. Moshchalkov, M. Baert, V. V. Metluskov, E. Rossell, M. J. Van Bael, K. Temst and Y. Bruynseraede, Phys. Rev. B 57, 3615, 1998.
- ¹⁶ V. Yurchenko, P. Lahl, S. Bunte, M. Jirsa and R. Wordenweber, Physica C 404, 426, 2004.
- ¹⁷ W. V. Pogosov and V. V. Moshchalkov, Physica C 404, 285, 2004.